Valence state partitioning of Cr and V between pyroxene - melt: Estimates of oxygen fugacity for martian basalt QUE 94201. J.M. Karner[1], (jkarner@unm.edu), J.J. Papike[1], C.K. Shearer[1], G. McKay[2], L. Le[2], and P. Burger[1]. [1] Astromaterials Institute, Dept. of Earth and Planetary Sciences, Univ. of New Mexico, Albuquerque, NM 87131. [2]Astromaterials Research Office, Mail Code KR, NASA JSC, Houston, TX, 77058.

Introduction: Several studies, using different oxybarometers, have suggested that the variation of fO_2 in martian basalts spans about 3 log units [e.g., 1-4] from ~IW-1 to IW+2. The relatively oxidized basalts (e.g., pyroxene-phyric Shergotty) are enriched in incompatible elements, while the relatively reduced basalts (e.g., olivine-phyric Y980459) are depleted in incompatible elements. A popular interpretation of the above observations is that the martian mantle contains two reservoirs; 1) oxidized and enriched, and 2) reduced and depleted [5]. The basalts are thus thought to represent mixing between these two reservoirs. Recently, Shearer et al. [6] determined the fO_2 of primitive olivine-phyric basalt Y980459 to be IW+0.9 using the partitioning of V between olivine and melt. In applying this technique to other basalts, [6] concluded that the martian mantle shergottite source was depleted and varied only slightly in fO_2 (IW to IW+1). Thus the more oxidized, enriched basalts had assimilated a crustal component on their path to the martian surface.

In this study we attempt to address the above debate on martian mantle fO_2 using the partitioning of Cr and V into pyroxene in pyroxene-phyric basalt QUE 94201. QUE 94201, along with Yamato 984059, are the best documented "melts" we have from the martian mantle. In other words, the rocks have experienced minimal accumulation or subtraction of phases, and more importantly the liquidus crystals formed in equilibrium with the bulk composition of the rock. Pyroxene is the first phase to crystallize in QUE 94201, and thus the partitioning of Cr and V between pyroxene cores and the bulk composition should lend insight into the fO_2 conditions under which the rock formed. This is possible because Cr and V are multivalent elements which are highly sensitive to the redox condition of a basaltic magma [7, 8], and thus partitioning of these elements into pyroxene is fO_2 dependent. It should be noted, however, that Cr and V partitioning into pyroxene are also dependent on Na and Al content [9, 10], which is why we use the QUE 94201 bulk composition for our experiments. For comparative purposes we also investigated Sc partitioning into pyroxene. Scandium exists as only Sc3+, and thus its partitioning should not be influenced by changes in fO_2.

Our procedure was to produce experimental charges of QUE 94201 composition at various fO_2 conditions and then compare the partitioning of Cr and V between pyroxene and bulk composition. Calibration curves of DCr, DV, and DCr/DV vs. fO_2 can then be used to calculate the fO_2 for the natural sample.

Experimental conditions: The starting material for the experimental runs was a synthetic glass having the same bulk composition as QUE 94201, spiked with 1000 ppm of V and Sc. Pressed pellets of the composition were first held for 48 hours at 1300 ºC in the 1 atm gas-mixing furnaces at JSC at imposed fO_2 conditions of IW-1, IW, IW+1, and QFM. The QFM runs produced olivine on the liquidus and thus were not used in this study. After quenching the charges to room temperature, the charges were then returned to their respective furnaces and cooled from a near liquidus temperature (1170 ºC) down to ~1100 ºC at a rate of 1 ºC/hr, and then quenched again. Pyroxene grains grown in the charges were first analyzed by electron microprobe for major and minor element composition, while V and Sc contents were determined by SIMS. Pyroxene grains in QUE 94201 were analyzed by the same protocol.

Results and Discussion: In all three charges (i.e., @ IW-1, IW, IW+1) pyroxene was the first phase on the liquidus and also the only phase to crystallize. All three charges produced Mg-rich pigeonite cores rimmed by Mg-rich augite. The crystallization trends and compositions of the experimental pyroxenes are shown in Figure 1. Also shown in Figure 1 are a small number of pyroxene compositions from QUE 94201. The pyroxenes in the natural sample are extremely complex and contain pigeonite and augite together in composite grains, but generally they show the same trends as the synthetic pyroxenes we produced, i.e., pigeonite rimmed by augite. Therefore, the best estimate of Cr and V partitioning between pyroxene and melt should be found in the Mg-rich pigeonite cores in both the experimental charges and the natural sample.

Analysis results of experimental and natural Mg-rich pigeonite for Cr, V, and Sc are listed in Table 1. Bulk Cr, V, and Sc were known for the experimental charges, while bulk values in QUE 94201 were taken from the literature [11]. Table 1. shows that in the experiments, DCr increases in pyroxene with increasing fO_2, while DV decreases with increasing fO_2. Over the same conditions, DSc essentially remains constant. These results make sense because Sc only exists in one valence state (3+), so fO_2 does not have an effect on its partitioning. Chromium exists as Cr2+ and Cr3+ depending on fO_2, and both may be in approximately

equal proportions in a basaltic melt equilibrated at an fO_2 of IW [10]. The increase in *D*Cr in pyroxene from IW-1 to IW+1 is the result of increasing fO_2 and subsequent increase of Cr3+/Cr2+ in the melt. Cr3+ is more compatible in the pyroxene structure than Cr2+ [10], and thus *D*Cr increases with increasing fO_2. Vanadium mainly exists as V3+ and V4+ at the fO_2 conditions of the experiments, and V3+ is more compatible in the pyroxene structure than V4+ [9, 10]. Consequently, a decreasing *D*V with increasing fO_2 reflects a lower V3+/V4+ in the crystallizing melt.

Figure 2 shows the *D*Cr, *D*V, and *D*Sc vs. fO_2 calibration curves derived from the experiment. Using the measured *D*Cr and *D*V for pyroxenes in QUE 94201, we obtain an fO_2 from the calibration curves of IW+0.2 and IW+0.9, respectively. Figure 2 also shows that *D*Sc forms a relatively flat curve for the experiments, and *D*Sc for the natural sample is similar to those values. In Figure 3 we ratio *D*Cr to *D*V to make another calibration curve. Applying the data from the natural sample to this curve we calculate an fO_2 of IW+0.6.

Conclusions: Based on *D*Cr and *D*V between pigeonite cores and bulk composition, we estimate QUE 94201 crystallized at an fO_2 between IW+0.2 and IW+0.9, with *D*Cr/*D*V suggesting IW+0.6. The strength of our fO_2 estimate is in our approach, because 1) the fO_2 is measured in the earliest crystallizing phase, 2) the calibration curves are based on the same bulk composition as the natural sample, and 3) that bulk composition represents a melt from the martian mantle, so true *D*Cr and *D*V are attainable. Presently, the two best candidates for martian melts, Y980459 and QUE 9420 indicate an fO_2 from IW to IW+1 for the upper martian mantle.

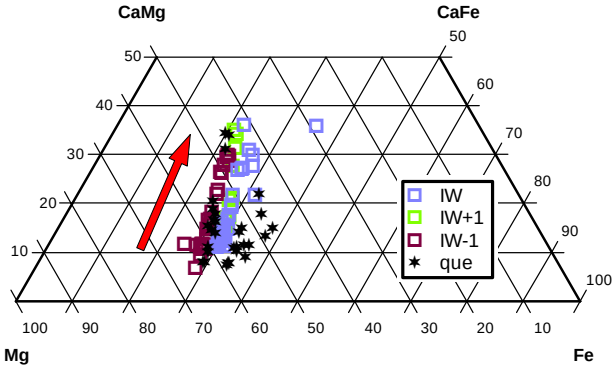

Figure 1. Pyroxene quad showing comparison of synthetic pyroxenes from this study with natural QUE 94201 pyroxenes. The red arrow indicates the direction of increasing crystallization.

Sample	fO_2	T °C	*D*Cr	*D*V	*D*Sc
QUE-exp26	IW+1	1170-1110	4.95	2.22	1.36
QUE-exp9	IW	1170-1100	4.27	2.87	1.27
QUE-exp10	IW-1	1170-1100	3.52	3.49	1.27
QUE 94201	DCr = IW+0.2 DV = IW+0.9 DCr/DV = IW+0.6	1170-	4.36	2.26	1.00

Table 1. Run conditions and analysis results for experimental and natural samples. QUE 94201 fO_2 determined by fitting *D*Cr and *D*V data to calibration curves (see Figure 2, 3).

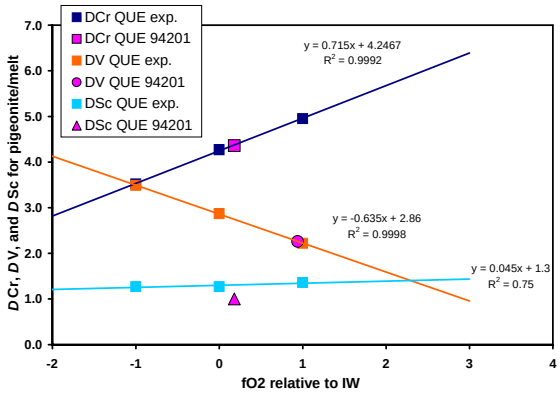

Figure 2. *D*Cr, *D*V, and *D*Sc vs. fO_2 for synthetic and natural QUE 94201 pyroxenes. *D*Cr and *D*V for natural sample are fit to the experimental curves, *D*Sc is simply placed at the calibrated *D*Cr fO2 value.

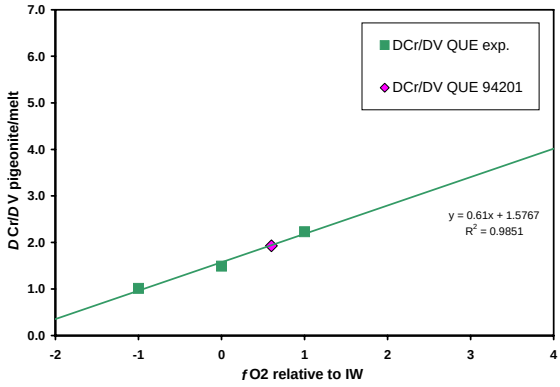

Figure 3. *D*Cr/*D*V vs. fO_2 for synthetic and natural QUE 94201 pyroxenes.

References: [1] Wadhwa (2001) Science, 291, 1527. [2] Herd et al. (2001) Am Min. 86, 1015. [3] McCanta et al. (2004) GCA 68, 1943. [4] Musselwhite et al. (2004) O in Terr. Plan. Wkshop, #3027. (CD-ROM) [5] Borg et al. (1997) GCA 61, 4915. [6] Shearer et al. (2006) Am Min. 91, 1657. [7] Hanson and Jones (1998) AmMin. 83, 669. [8] Karner et al. (2006) AmMin. 91, 270. [9] Karner et al. (2006) AmMin 91, 1574. [10] Papike et al. (2005) *AmMin* 90, 277. [11] Warren et al. (1996) Proc. NIPR 21, 195.

Acknowledgements: This research was funded by a NASA cosmochemistry grant to JJP.